Femtochemistry

The Transition State of Thermal Organic Reactions: Direct Observation in Real Time**

*D. Hern Paik, Ding-Shyue Yang, I-Ren Lee, and Ahmed H. Zewail**

The motion of atoms during chemical reactions occurs on the femtosecond time scale, and only with this resolution can the transition state be frozen in time. Numerous examples of femtochemistry studies have been reported for reactions on excited surfaces and in all phases of matter (see, for example, recent references [1] and [2]). Combining the femtosecond time resolution and negative-ion-beam techniques provides a unique way to study the nuclear motions of *neutral* molecules in the electronic *ground* state, and this has been successful for Ag_3 and Ag_4.[3–7]

For stable (positive electron affinity) negative ions prepared in the gas phase the electronic states are lower in energy than the neutral ground state. Thus, the ground state of the neutral reaction can be prepared with well-defined nuclear configuration (coherent wave packet) by photodetaching the electron from the anion with a femtosecond laser pulse. Because the geometries of the anion and the neutral molecule are different, the vertical transition results in significant nuclear motion toward the equilibrium geometry of the ground state. This motion can be monitored in real time by using a second femtosecond laser pulse, with variable time delay, through ionization and detection with mass spectrometry.

---

[*] D. H. Paik, D.-S. Yang, I-R. Lee, Prof. Dr. A. H. Zewail
Laboratory for Molecular Sciences
Arthur Amos Noyes Laboratory of Chemical Physics
California Institute of Technology
Pasadena, CA 91125 (USA)
Fax: (+1) 626-792-8456
E-mail: zewail@caltech.edu

[**] Financial support from the National Science Foundation is acknowledged.

DOI: 10.1002/ange.200453962

In the present work we report the femtosecond (fs) time-resolved dynamics of the transition state of the reaction of 1,3,5,7-cyclooctatetraene (COT) [Eq. (1)]. This reaction of

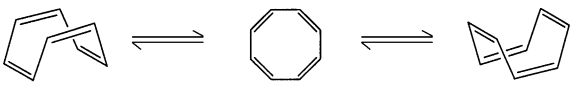
(1)

neutral COT on the ground-state potential is not a photochemical one, thus the transition state is that of a thermal reaction.

For this system a number of experimental and theoretical works have shown that neutral COT has a "tub-shaped" (D_{2d}) structure in the electronic ground state,[8–16] whereas the COT anion has a planar (D_{4h}) structure that resembles the geometry of neutral COT at the transition state of the ring inversion.[17–21] From the photoelectron spectrum of COT$^-$, Wenthold et al. showed that the vertical transition from COT$^-$ can directly access the transition state of the ring inversion in the electronic ground state of neutral COT.[20]

In our experiment the coherent wave packet of the nuclear motion was launched from the negative ion using a 405-nm femtosecond pulse (Figure 1). The COT$^-$ ion was mass-selected (Figure 2 a), and the pump pulse (3.1 eV) photodetaches the electron from the anion to yield the transition state (TS) of the neutral reaction. The released electron carries most of the energy, and the wave packet is launched directly at the transition state (Figure 1). We then ionized the neutral COT with two photons of the probe pulse (270 nm) with variable time delay and monitored the temporal evolution of the mass spectrum of COT$^+$ (Figure 2 c).

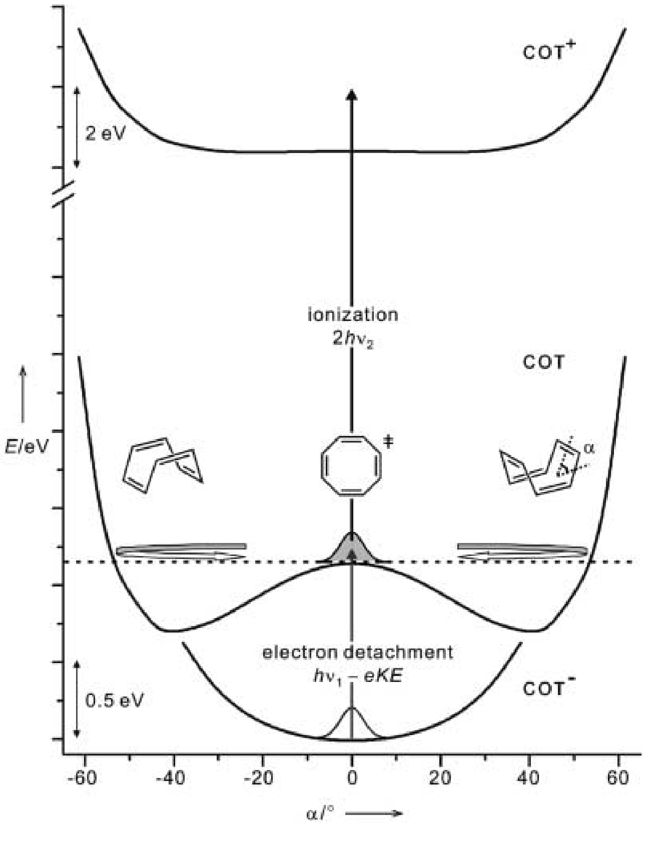

Figure 1. Schematic illustration of the experiment, with calculated potential energies for COT$^-$, COT, and COT$^+$ as a function of the bending angle (α). The electron detachment by the pump pulse and ionization by the probe pulse are indicated by upward arrows. The initial wave packet prepared by the pump pulse is indicated by a Gaussian profile at the transition state of the ring inversion.

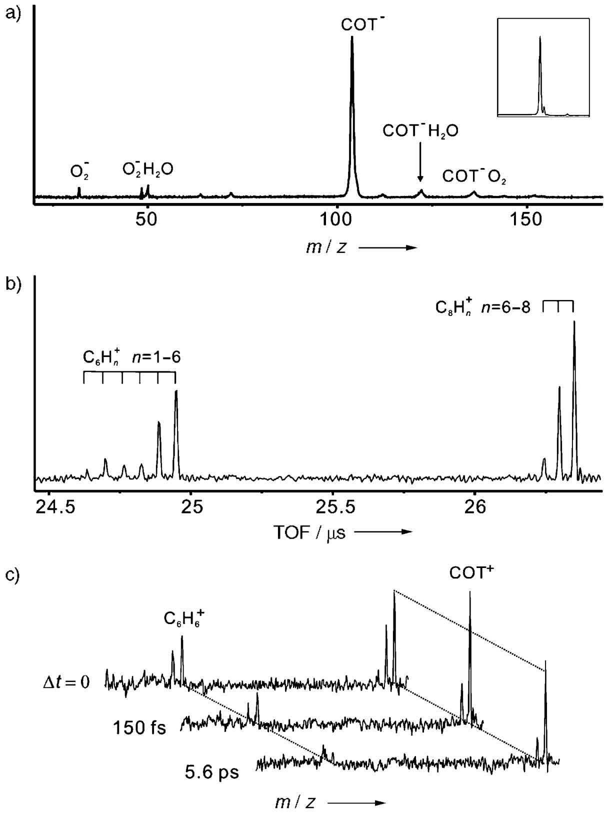

Figure 2. a) Mass spectrum of negative ions produced by the electron-impact source. Inset: High-resolution mass spectrum obtained by the linear reflectron mass spectrometer. b) Positive-ion time-of-flight (TOF) mass spectrum generated by intercepting COT$^-$ with the pump and probe pulses at 160 fs. c) Time-dependent mass spectra of the positive ions obtained at three different delay times (0, 160 fs, and 5.6 ps), which display the increment of the positive-ion signals with respect to the reference at −1 ps $[I(t)-I_{t<0}]$. With the pump and probe pulses we always observed enhancement of fragment cations as well as the parent COT$^+$ at all positive delay times. Thus, the enhanced COT$^+$ signal is due to the generation of neutral COT by the pump pulse at positive delay rather than from the depletion of the background COT$^+$ at negative delay. For the latter, the fragment-ion signal should appear as a dip in the difference spectrum. Note that the peak for COT$^+$ first increases and then decreases with time (see Figure 3).

The mass spectrum of negative ions is shown in Figure 2 a, together with the high-resolution peak obtained by the linear reflectron mass spectrometer. The photoelectron (PE) spectrum (not shown) of COT$^-$ for detachment at 405 nm with a femtosecond pulse is consistent with that reported by the Lineberger group.[20] Our spectrum shows the main peaks, but the broadening is mainly due to the Doppler effect in the magnetic-bottle detection;[22] in our ion source some minor intensity (hot bands) was observed at the <1-eV threshold. The important point is that the PE spectrum displays the electron detachment to both the singlet (1.1 eV) and triplet (1.6 eV) states.

Figure 2b shows the positive-ion time-of-flight mass spectrum obtained by using the two femtosecond pulses at a positive delay time. Under our experimental conditions COT^+ was generated even with the probe pulse alone, but this resulted in a background signal. However, when both the photodetaching pump pulse and the ionizing probe pulse were temporally synchronized, we observed the transient behavior in the mass spectrum of the positive ions shown in Figure 2c for the three delay times 0 fs, 160 fs, and 5.6 ps.

In order to follow the temporal evolution, we recorded many such transients, and the behavior is shown in Figure 3 for gating at the mass of COT^+. The observed transient exhibits two characteristics: 1) positive signal offset (shown by a thin line) and 2) an apparent damped oscillatory behavior. The positive offset is understood because the detachment of electron from COT^- yields both the singlet and triplet states of COT, as evident in the PE spectrum. The offset is flat within 4 ps (Figure 3) and up to 12 ps (not shown), and this is consistent with a contribution from a long-lived triplet state ($\approx 100\ \mu s$).[23]

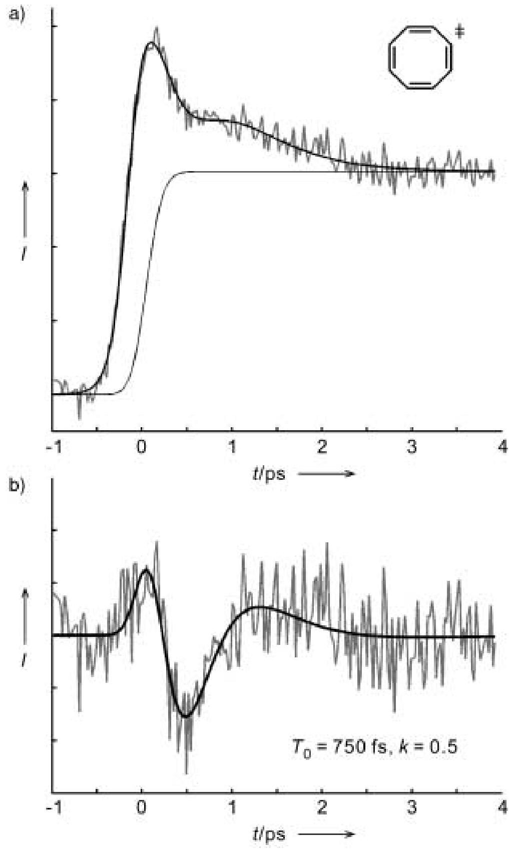

Figure 3. Transition-state dynamics of ground-state COT. Femtosecond transients of COT generated by the pump–probe scheme described in Figure 1 and gated using the COT^+ ion signal. a) The measured transient is shown together with the theoretical fit of Equation (2). The oscillatory feature ($a=0$) is illustrated in b (see text for details). There is a small contribution at negative time because of the reverse "probe–pump" signal. This is clear in our analysis because the initial peak is a factor of two broader than our cross correlation.

The oscillatory behavior is reminiscent of the transient behavior observed by our research group for the photoisomerization of *cis*-stilbene.[24] The transient fit shown in Figure 3 was obtained using the molecular-response function with proper convolution given in Equation (2), where γ is the

$$M(t) = \exp(-\gamma t) \cdot \{a + b \cdot \cos[\omega(t)t]\} \tag{2}$$

decay rate and a and b are constants. The time-dependent frequency is $\omega(t) = 2\pi/(T_0 + kt)$, where T_0 is the initial period and k gives its change (dispersion) with time. From the fit we obtained $\gamma^{-1} = 750$ fs, $a/b = 2.6$, $T_0 = 750$ fs, and $k = 0.5$. The residual sinusoidal component ($a=0$) is shown in Figure 3b.

These results indicate that the prepared wave packet of COT nuclear motions (the planar structure of the TS) initially decays (and dephases) on a time scale similar to the oscillatory period between the two tub-shaped structures. Also, as the wave packet moves away from the TS the period increases by 50% in 750 fs.

In order to elucidate the nature of the oscillatory motion on the ground-state surface, we first carried out a quantum simulation of wave-packet trajectory along the one-dimensional ring inversion (Figure 1). The potential energy curve was calculated using density functional theory, and we obtained all normal modes at different geometries including the ring inversion of imaginary frequency. Regardless of the probe-window position, we obtained a recurrence period of ≈ 350 fs, which is about half of our experimental value. This large discrepancy led us to examine the importance of the multidimensional energy landscape in view of the fact that transverse (to the TS) mode(s) can be very important.

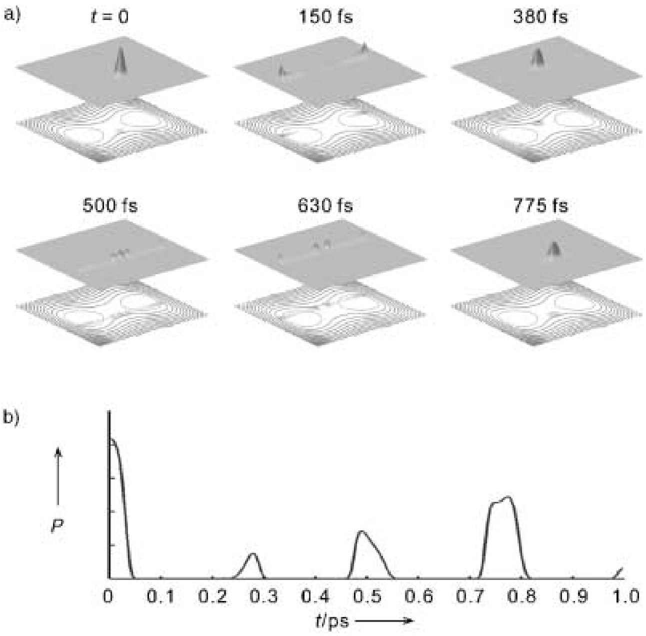

Figure 4. a) Snapshots of wave-packet evolution on the two-dimensional contour (RI1, RI2). Note that the wave packet returns to the initial position at 775 fs. b) The simulated molecular-response function obtained by opening the probe window at the initial wave-packet position. P = probability.

On a two-dimensional surface, which includes both the reaction coordinate for ring inversion (RI1) and a second coordinate whose frequency is close to that of another ring inversion (RI2, $\approx 200\,\mathrm{cm^{-1}}$), we obtained the snapshots shown in Figure 4; the RI1 and RI2 coordinates correspond to the flipping motions along the double and single bonds, respectively (Figure 5). From these quantum calculations we plotted the probability as a function of time, with the detection window located at the TS launching position.[25] We can see that the prominent wave-packet period is now in agreement with experiment (775 fs). However, we must account for the selectivity imposed on the window of detection along the harmonic transverse mode (RI2). This asymmetry of detection can be rationalized by considering the multiple transition states shown in Figure 5. COT, through bond shifting (BS, $\approx 1700\,\mathrm{cm^{-1}}$; 20 fs), can acquire a D_{8h} TS which is located only 4 kcal mol^{-1} from the D_{4h} geometry.[19] As shown in Figure 5, this ultrafast interconversion can induce such asymmetry. The two lowest frequency normal modes (degenerate E_{2u}) at the D_{8h} geometry are the linear combination of the first (reaction coordinate) and the second ring-inversion modes, which suggests that Duschinsky rotation plays an important role, especially at the transition state of the reaction coordinate.[26]

In conclusion, we have demonstrated real-time probing of the transition-state dynamics of cyclooctatetraene in the electronic ground state. This transition state is unique in its definition for thermal reactions, and here it was directly accessed by detachment of the electron from the planar COT$^-$ anion. The motion in the multidimensional nuclear space in the reaction of neutral COT was monitored by ionization/mass spectrometry. The oscillatory feature observed in the transients reflects trajectories of motion (resonance) along the reaction coordinate, the ring-inversion motion. With the aid of quantum calculations we examined the nature of the modes involved and the energy landscape. It should now be possible to apply this methodology to other ground-state thermal reactions for the real-time probing of their transition states.

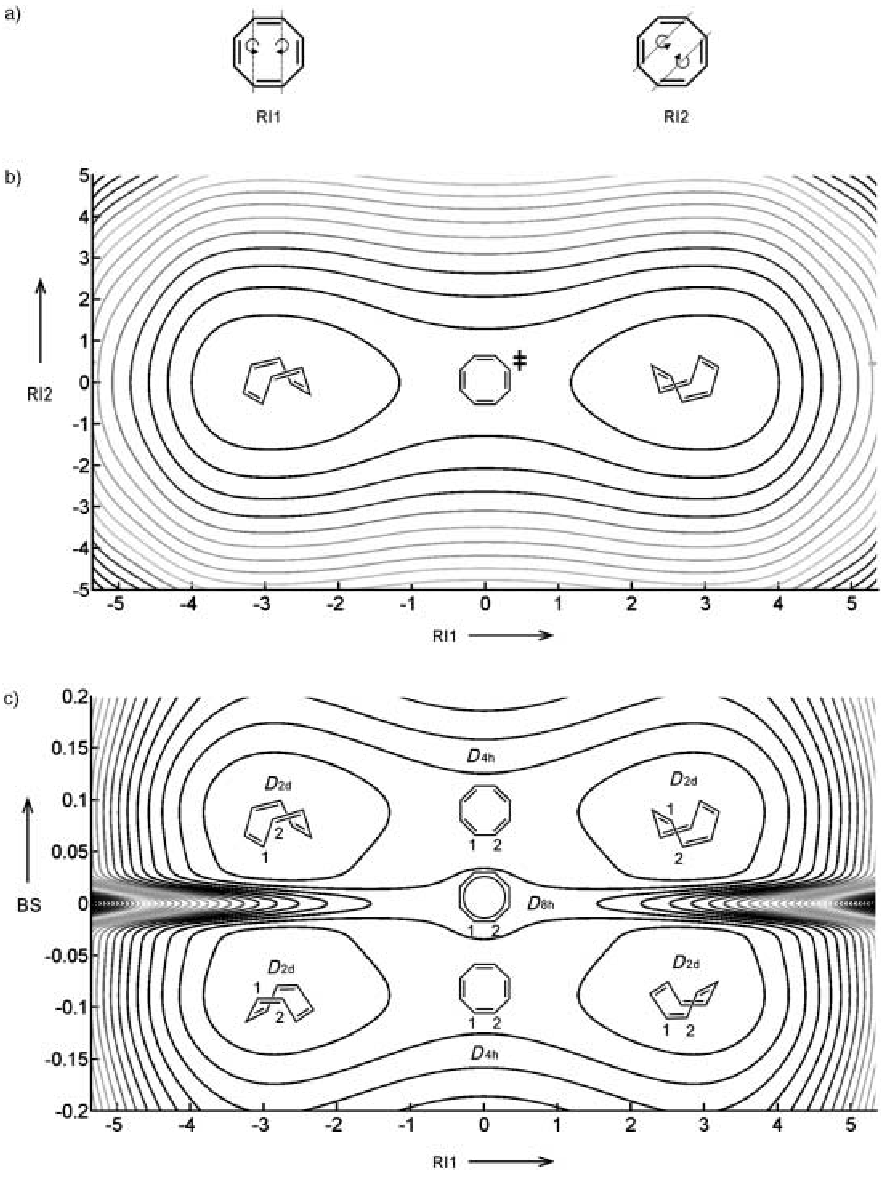

Figure 5. a) Representation of the two coordinates of ring inversion. b) Two-dimensional representation of the potential-energy surface of the electronic ground state along RI1 and RI2. The contour is constructed by adding two one-dimensional curves. c) Potential contours schematic along the ring inversion RI1 and bond-shifting (BS) coordinates.

Experimental Section

The ion-beam apparatus was described elsewhere.[27] Briefly, COT$^-$ was generated by crossing a $\approx$1-keV electron pulse with the gaseous mixture of COT/O_2/Ar. The COT vapor at 25 °C was expanded into a high-vacuum chamber by flowing through premixed Ar/O_2 gas (approximately 95 % Ar and 5 % O_2) at a total backing pressure of 400 psig. A small amount of O_2 was introduced in the gas line, which produced more COT$^-$ and stabilized the ion intensity. The ion beam was collimated by a skimmer (1.0-mm hole) and then directed into the field-free time-of-flight region by applying a −3.0-kV electric pulse to a two-stage accelerator. In the field-free region, ions were separated by their masses, and the anion packet of COT$^-$ was intercepted with femtosecond laser pulses by adjusting the switching time of the ion accelerator with respect to the laser arrival time.

The femtosecond laser pulses (110 fs) at 810 nm and 820 nm were generated from a Ti:sapphire oscillator and amplified by the regenerative and the two-stage multipass amplifiers. The IR fundamental was split (50:50), and one of the beams was frequency-doubled. The other beam was converted to the third harmonic by sequential doubling and sum-frequency mixing. The second harmonic (405 nm or 410 nm) was used as the pump pulse to photodetach the electron from COT^-, and the third harmonic (270 nm or 273 nm) was used as the probe pulse to ionize the nascent neutral COT by two-photon absorption. Positive ions generated in the laser-interaction region were collected by the reflectron mass spectrometer, and the detached electron was analyzed by the magnetic-bottle PE spectrometer. Time-dependent transient was obtained by integrating the COT^+ ion peak as a function of the delay time between the pump and probe pulses (cross correlation 300 fs).

Ab initio calculations for the potential energy along the reaction coordinate (RI1) were made using the Gaussian 98 program at the B3LYP/cc-pVTZ level of theory.[28] Wave-packet motions were calculated by numerically solving the Schrödinger equation.

Received: February 6, 2004 [Z53962]

Keywords: cyclooctatetraene · femtochemistry · photodetachment · transition states · wave-packet dynamics

---

[1] *Femtochemistry and Femtobiology* (Eds.: A. Douhal, J. Santamaria), World Scientific, River Edge, New Jersey, **2002**.

[2] *Femtochemistry: with the Nobel Lecture of A. Zewail* (Eds.: F. S. De Schryver, S. De Feyter, G. Schweitzer), Wiley-VCH, Weinheim, **2001**.

[3] S. Wolf, G. Sommerer, S. Rutz, E. Schreiber, T. Leisner, L. Wöste, R. S. Berry, *Phys. Rev. Lett.* **1995**, *74*, 4177 – 4180.

[4] D. W. Boo, Y. Ozaki, L. H. Andersen, W. C. Lineberger, *J. Phys. Chem. A* **1997**, *101*, 6688 – 6696.

[5] M. Hartmann, J. Pittner, V. Bonačić-Koutecký, A. Heidenreich, J. Jortner, *J. Chem. Phys.* **1998**, *108*, 3096 – 3113.

[6] I. Andrianov, V. Bonačić-Koutecký, M. Hartmann, J. Manz, J. Pittner, K. Sundermann, *Chem. Phys. Lett.* **2000**, *318*, 256 – 262.

[7] H. Hess, K. R. Asmis, T. Leisner, L. Wöste, *Eur. Phys. J. D* **2001**, *16*, 145 – 149.

[8] F. A. L. Anet, *J. Am. Chem. Soc.* **1962**, *84*, 671 – 672.

[9] M. Trætteberg, *Acta Chem. Scand.* **1966**, *20*, 1724 – 1726.

[10] R. P. Frueholz, A. Kuppermann, *J. Chem. Phys.* **1978**, *69*, 3614 – 3621.

[11] D. A. Hrovat, J. H. Hammons, C. D. Stevenson, W. T. Borden, *J. Am. Chem. Soc.* **1997**, *119*, 9523 – 9526.

[12] C. D. Stevenson, E. C. Brown, D. A. Hrovat, W. T. Borden, *J. Am. Chem. Soc.* **1998**, *120*, 8864 – 8867.

[13] J. L. Andrés, O. Castaño, A. Morreale, R. Palmeiro, R. Gomperts, *J. Chem. Phys.* **1998**, *108*, 203 – 207.

[14] O. Castaño, R. Palmeiro, L. M. Frutos, J. Luisandrés, *J. Comput. Chem.* **2002**, *23*, 732 – 736.

[15] M. Garavelli, F. Bernardi, A. Cembran, O. Castaño, L. M. Frutos, M. Merchán, M. Olivucci, *J. Am. Chem. Soc.* **2002**, *124*, 13770 – 13789.

[16] L.-M. Frutos, O. Castaño, M. Merchán, *J. Phys. Chem. A* **2003**, *107*, 5472 – 5478.

[17] M. J. S. Dewar, A. Harget, E. Haselbach, *J. Am. Chem. Soc.* **1969**, *91*, 7521 – 7523.

[18] R. Gygax, H. L. McPeters, J. I. Brauman, *J. Am. Chem. Soc.* **1979**, *101*, 2567 – 2570.

[19] J. H. Hammons, D. A. Hrovat, W. T. Borden, *J. Am. Chem. Soc.* **1991**, *113*, 4500 – 4505.

[20] P. G. Wenthold, D. A. Hrovat, W. T. Borden, W. C. Lineberger, *Science* **1996**, *272*, 1456 – 1459.

[21] T. M. Miller, A. A. Viggiano, A. E. S. Miller, *J. Phys. Chem. A* **2002**, *106*, 10200 – 10204.

[22] H. Handschuh, G. Ganteför, W. Eberhardt, *Rev. Sci. Instrum.* **1995**, *66*, 3838 – 3843.

[23] T. N. Das, K. I. Priyadarsini, *J. Chem. Soc. Faraday Trans.* **1994**, *90*, 963 – 968.

[24] S. Pedersen, L. Bañares, A. H. Zewail, *J. Chem. Phys.* **1992**, *97*, 8801 – 8804.

[25] The largest ion signal was observed at time-zero (Figure 3) suggesting the probing from the initial launched configuration. It should be noted that when the photodetachment (ionization) of the electron is on a time scale shorter than that of the nuclear motion, then Franck–Condon vertical transitions become an appropriate description of the transitions.[29] To map out the different positions along the reaction coordinate[30] one must consider the change in the transition probability.

[26] D. A. Hrovat, W. T. Borden, *J. Am. Chem. Soc.* **1992**, *114*, 5879 – 5881.

[27] D. H. Paik, N. J. Kim, A. H. Zewail, *J. Chem. Phys.* **2003**, *118*, 6923 – 6929.

[28] Gaussian 98 (Revision A.9), M. J. Frisch, G. W. Trucks, H. B. Schlegel, G. E. Scuseria, M. A. Robb, J. R. Cheeseman, V. G. Zakrzewski, J. A. Montgomery, R. E. Stratmann, J. C. Burant, S. Dapprich, J. M. Millam, A. D. Daniels, K. N. Kudin, M. C. Strain, O. Farkas, J. Tomasi, V. Barone, M. Cossi, R. Cammi, B. Mennucci, C. Pomelli, C. Adamo, S. Clifford, J. Ochterski, G. A. Petersson, P. Y. Ayala, Q. Cui, K. Morokuma, D. K. Malick, A. D. Rabuck, K. Raghavachari, J. B. Foresman, J. Cioslowski, J. V. Ortiz, B. B. Stefanov, G. Liu, A. Liashenko, P. Piskorz, I. Komaromi, R. Gomperts, R. L. Martin, D. J. Fox, T. Keith, M. A. Al-Laham, C. Y. Peng, A. Nanayakkara, C. Gonzalez, M. Challacombe, P. M. W. Gill, B. G. Johnson, W. Chen, M. W. Wong, J. L. Andres, M. Head-Gordon, E. S. Replogle, J. A. Pople, Gaussian, Inc., Pittsburgh, PA, **1998**..

[29] Y. Arasaki, K. Takatsuka, K. Wang, V. McKoy, *J. Chem. Phys.* **2003**, *119*, 7913 – 7923.

[30] A. Mokhtari, P. Cong, J. L. Herek, A. H. Zewail, *Nature*, **1990**, *348*, 225 – 227.